Systematics in the Electronic Spectra of Polar Molecules. 2. Ortho- and Meta-Disubstituted Benzenes

G. L. Findley, T. P. Carsey, and S. P. McGlynn*

Contribution from the Choppin Chemical Laboratories, The Louisiana State University, Baton Rouge, Louisiana 70803. *Received November 13, 1978*

Abstract: The absorption and emission properties of ortho- and meta-disubstituted benzenes, one substituent being an electron acceptor and the other an electron donor, are discussed from computational (CNDO/s) and experimental points of view. It is found that $E(^1L_a)$ or $E(^1L_b)$ serves to parametrize the degree of charge transfer in the respective states. Unlike the para isomers, $E(^1L_a) - E(^1L_b)$ is always positive and approximately 10 000 cm^{-1}. The T_1 state is always ^3L_a. The gamut of properties which are mediated by an increasing degree of charge transfer are elaborated and are interpreted (and also interrelated with those of the para isomers) using the computational data. Particular attention is paid to the interrelationship of emissive and absorptive properties. It is found that $^1L_b/^1CT$ mixing in the ortho and meta isomers induces considerable dipole allowedness in their ^1L_b states whereas the same mixing in the para isomer is much less efficient in conferring dipole allowedness on its ^1L_b state.

Introduction

The electronic absorption spectra of the positional isomers of any disubstituted benzene D-Ph-A, where D is an electron-donor substituent and A an electron-acceptor substituent, exhibit a striking characteristic. The spectra of the ortho and meta isomers are quite similar, and very different from that of the para isomer. This characteristic, to which we refer henceforth as characteristic A′, is very evident in Figure 1. The interpretation of characteristic A′ was first given by Murrell and Nagakura using an intramolecular charge transfer (CT) model.[1] Indeed, the success of this interpretation had much to do with the ensuing popularity of such CT models.

The absorption spectra of Figure 1 are arranged, left to right, in the order of increasing D/A index of the donor and acceptor substituents.[2] In addition to characteristic A′, which is particularly obvious, even the most cursory inspection of Figure 1 suggests the existence of a number of other regularities which, in some way, are gauged by the D/A index. However, little effort seems to have been invested in the elaboration of these other regularities. Consequently, a principal aim of this work is the delineation of such absorptive characteristics and their dependency on the D/A index.

Even less attention has been paid to the emissive properties of these molecules. Yet, as shown in Figure 2, a good deal of behavioral regularity is also evident in the luminescence spectra. For example, the emission spectroscopic counterpart of characteristic A′ clearly exists, and, in view of the D/A gauging of many of the absorptive properties, some of the other emission characteristics might even have been predicted. Consequently, another aim of this work is the elaboration of the parametric dependence of luminescence characteristics on the D/A index, and the rationalization of this dependence in terms of the absorptive properties.

The investigative approach adopted is identical with that of the previous paper[3] (which, henceforth, we denote I). Interest resides in the regular dependence of the electronic spectroscopic properties on some ordering parameter, say the D/A index, and not in the peculiarities of any one compound, regardless of how bizarre those peculiarities might be. The approach, in other words, is correlative, and, as in I, it will make extensive use of computational (ASMO-CI) and experimental data.

In order to proceed further, however, it is necessary to append labels to the various excited electronic states of the ortho and meta isomers. The labels used are those appropriate to the para isomers of I, namely, $^{1,3}L_{a,b}$ and $^{1,3}B_{a,b}$. However, the minimal point group symmetry for which these symbolics are meaningful is C_{2v} whereas all the ortho and meta isomers discussed here belong to C_s point groups. In other words, the absence of symmetry-defined "long" and "short" molecular axes in the ortho and meta isomers forces the use of an inappropriate, perhaps even wrong, notation. We assert, despite this, that the notation is meaningful, even if only in an *evolutionary* sense. This assertion is justified on the basis of the following computational results: (1) the manner in which the energies and oscillator strengths of various $^1\Gamma_{\pi\pi^*} \leftarrow {}^1\Gamma_1$ transitions evolve from those of benzene (which will be made correlatively evident in the section entitled "Quantum Chemical Correlations") [In view of that result, it is convenient, for example, to use the label ^1L_a, thereby implying that the state in question evolves into the corresponding benzenoid state in the limit in which the D/A index approaches zero.]; (2) the manner in which the theoretical configurational descriptions, at the Slater determinant level, evolve into those of an innocuously substituted benzene at the same limit of the D/A index; (3) the consistency with which the two lowest energy $^3\Gamma_{\pi\pi^*}$ configurations relate to the two lowest energy $^1\Gamma_{\pi\pi^*}$ configurations and the fact that these relations are identical with those in the para isomers.

Hence, we use the ($^{1,3}L_{a,b}$, $^{1,3}B_{a,b}$) notation with impunity. However, we reemphasize that this use is valid only in an evolutionary sense, and that, applied to one individual ortho or meta isomer (particularly one of large D/A index), it is totally devoid of meaning. In other words, this notation is meaningful in a correlative manner since, in that case, it connotes a limiting procedure.

Quantum Chemical Correlations

A limited data set suffices to illustrate the general trends exhibited by the ortho and meta isomeric sets. The molecules in this limited set are shown in Figure 3.

1. Dipole Moments. The ground-state dipole moments, evaluated in the point charge approximation,[4] are given in Table I. The order in which the dipole moments increase is the same in both the computational and the experimental data sets (where the latter data exist). Furthermore, this order is identical with that of the D/A index expected on the basis of qualitative considerations. Consequently, we conclude that μ_0 constitutes a rough gauge of the D/A index.

The simple vector model, which predicts ratios $1:\sqrt{3}/2:1/\sqrt{2}$ for μ_0 (para):μ_0(meta):μ_0(ortho), is obviously invalid. Indeed, μ_0 lies more or less along the axis defined by the strong donor (acceptor) group when the conjugate acceptor (donor) group is weak. Hence, the only significant deviation

0002-7863/79/1501-4511$01.00/0

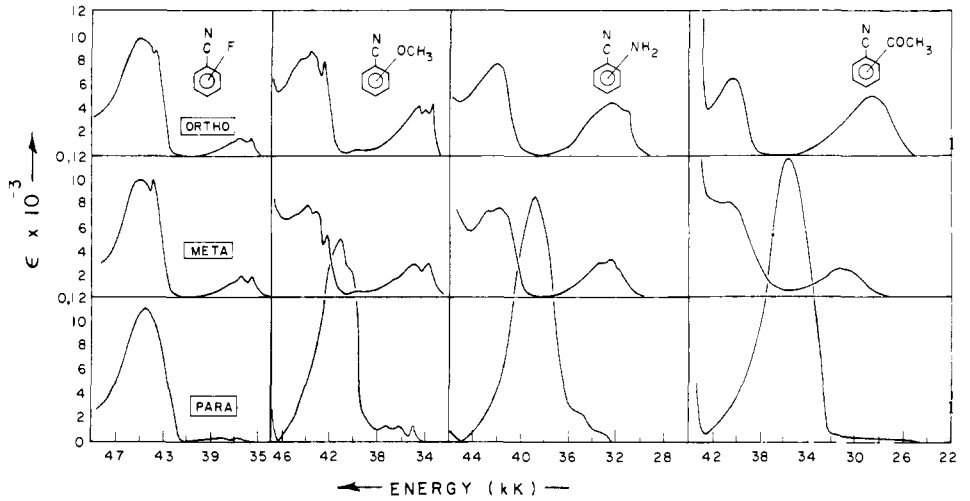

Figure 1. The absorption spectra of a representative set of ortho/meta/para isomeric triads D-Ph-A arranged in order top/middle/bottom. The arrangement left to right is that of an increasing D/A index[2] (or molecular polarity). The solvent was either methylcyclohexane or isopentane; the temperature was 300 K. The molar decadic extinction coefficient ϵ is cited in units L/mol·cm.

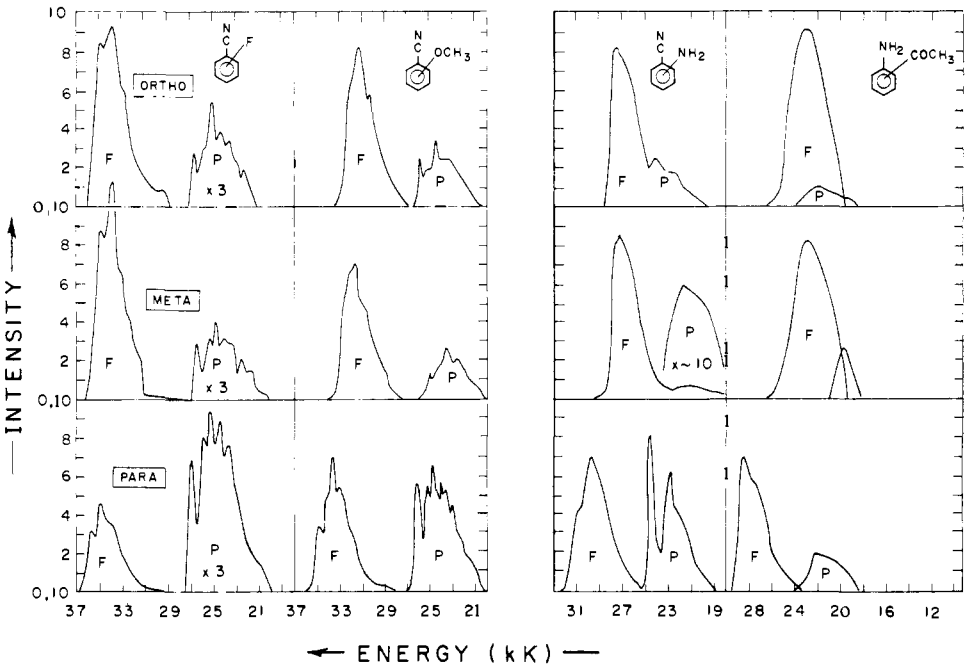

Figure 2. The luminescence spectra (corrected) of a representative set of ortho/meta/para isomeric triads D-Ph-A arranged in order top/middle/bottom. The arrangement left to right is that of an increasing D/A index[2] (or molecular polarity). The solvent was EPA; the temperature was 77 K. Fluorescence is denoted F and phosphorescence is denoted P. The phosphorescence/fluorescence intensites within any one block are relatively correct but are otherwise arbitrary.

of dipole direction occurs in *o*- and *m*-cyanophenols, where donor and acceptor groups are of comparable strength. In all other instances, the acceptor dominates, and defines the dipole direction.[5]

2. Energies and Oscillator Strengths. These computed quantities are plotted in Figures 4 (ortho isomers) and 5 (meta isomers). The left-to-right arrangement of molecules in Figures 4 and 5 is that of increasing μ_0. The correlation lines imposed on these figures are self-evident. Comparison of Figures 4 and 5 of this work with Figure 2 of I indicates the following regularities.

(A) Characteristic A, congruent with A′, exists and is more pronounced at large D/A index.

(B) The energies $E(^1L_a)$ and $E(^1L_b)$ decrease as μ_0 increases. Consequently, $E(^1L_a)$ may serve as a gauge, although a less sensitive one than $E(^1L_a)$ of the para set, of the D/A index.

(C) The ^1L_a-^1L_b band gap remains almost constant at ~8 × 10^3 cm^{-1}. This behavior contrasts markedly with the ^1L_a/^1L_b crossover of the para set.

(D) The ^1L_a-^3L_a band gap decreases regularly as μ_0 increases. This decrease is less precipitous than in the para set. The ostensible reason for this lesser sensitivity is the lesser degree of CT character infused into the ^1L_a state of the ortho and meta sets relative to the para set.

(E) The oscillator strength[8] $f(^1L_a)$ decreases and $f(^1L_b)$ increases with increasing μ_0. The ratio $f(^1L_b)/f(^1L_a)$ exhibits a very regular but moderate increase, in marked contrast to the apparent decrease of the same ratio in the para set. The reason for this behavior is the rather large component of CT character (CT character such that $^1\Gamma_{CT} \leftarrow {}^1\Gamma_1$ is strongly dipole allowed) which is infused into the ^1L_b state of either an ortho or meta isomer. Such an infusion of a "strongly allowed $^1\Gamma_{CT}$ state" into the ^1L_b state of the para isomer does not occur.

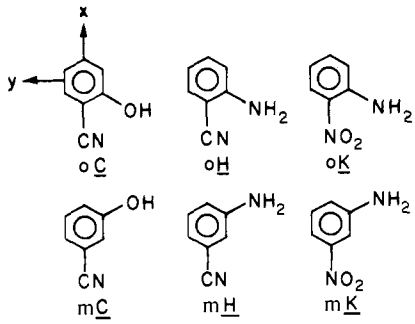

Figure 3. The set of molecules for which computational data are reported. All molecules belong to the C_s point group. The indexes C, H, and K are identical with those used in I (see Figure 1 of I). Prefixes *o* (ortho) or *m* (meta) have been added for convenience. The structural references are *o*C, *o*H, *m*C, and *m*H (ref 6); *o*K and *m*K (ref 7).

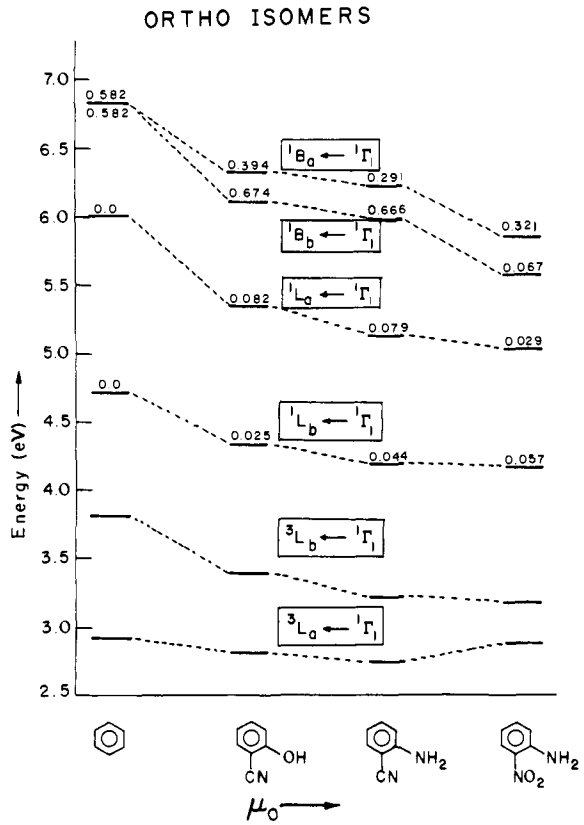

Figure 4. Energies and oscillator strengths of the low-energy $^{1,3}\Gamma_{\pi\pi^*} \leftarrow {}^1\Gamma_1$ transitions of a representative set of *o*-D-Ph-A molecules. All quantities were calculated by CNDO/s-CI procedures.

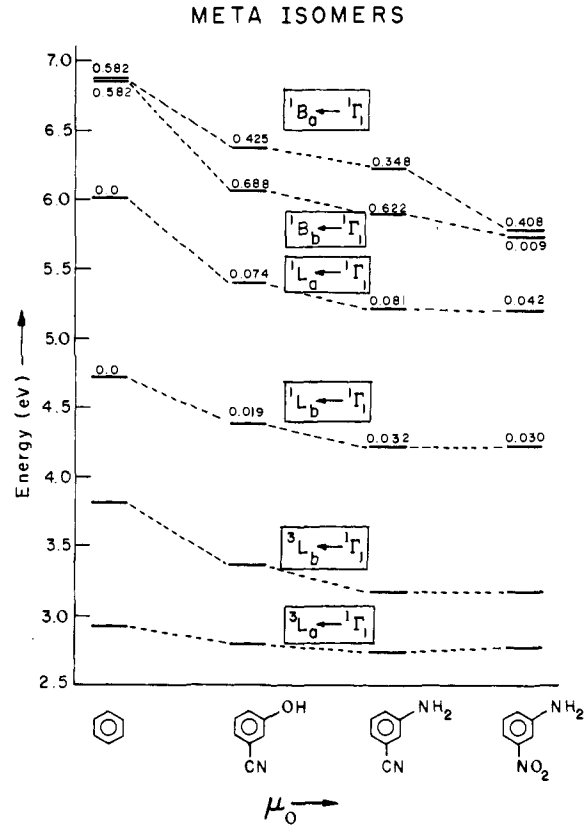

Figure 5. Energies and oscillator strengths of the low-energy $^{1,3}\Gamma_{\pi\pi^*} \leftarrow {}^1\Gamma_1$ transitions of a representative set of *m*-D-Ph-A molecules. All quantities were calculated by CNDO/s-CI procedures.

Table I. Calculated and Experimental Values of the Ground-State Dipole Moment (D)[a]

molecule	isomer	μ_0 (calcd)	μ_0 (exptl)	angle
cyanophenol	*o*	2.26		−3° 57′
	m	2.24		−8° 28′
	p	2.94	4.95	−11° 8′
cyanoaniline	*o*	2.51		−23° 22′
	m	3.32		−15° 51′
	p	3.96	5.96	0°
nitroaniline	*o*	5.02	4.06	−3° 13′
	m	5.75	4.89	−2° 41′
	p	6.45	6.31	0°

[a] These molecules are shown in Figure 3. The experimental values are taken from McClelland (A. L. McClelland, "Tables of Experimental Dipole Moments", W. H. Freeman, San Francisco, 1963). They refer to dielectric constant data in a benzene solvent. The angle is measured with respect to the *x* axis of Figure 3.

Indeed, if one supposes that $f(^1L_a)$ of para is merely redistributed over both $f(^1L_a)$ and $f(^1L_b)$ of ortho (or meta), one concludes that $f(^1L_a) + f(^1L_b)$ for ortho (or meta) should equal $\sim 0.5 f(^1L_a)$ of para. The observed ratio, remarkably constant in all three D-Ph-A sets, is ~0.35.

3. Charge Transfer. The degree of CT in the ^1L_a and ^1L_b states of an ortho or meta isomer may not be usefully discussed[3] in terms of $F_A + F_D$ of I. The charge increments or decrements of the groups A and D, respectively, are inadequate for a specification of the total charge displacements which accompany a given electronic excitation process because the phenyl moiety may also function as a donor, relative to A, or as an acceptor, relative to D. In consequence of this, the analysis of the CT character of a given state is somewhat ambiguous and we will content ourselves here with the statement that the degree of CT of types D^+-Ph-A^-, D-Ph$^+$-A^-, and D^+-Ph-A^- is comparable in both the ^1L_a and ^1L_b states of the ortho and meta isomers and that it is this facet of the electronic structure that accounts for the ortho/meta similarity part of characteristic A′.

Experimental Correlations

A correlation of the experimental data is given in Figure 6 for the ortho isomers and in Figure 7 for the meta isomers. The molecules of Figures 6 and 7 are ranked horizontally in the order of decreasing $E(^1L_a)$ and contain variable acceptor and donor groups. Plots of the same type, but ranked according to μ_0 and with (fixed D, variable A) and (fixed A, variable D) substituents, are available elsewhere.[9] These latter plots demonstrate the relevance of the μ_0 gauge of both D/A index and $E(^1L_a)$, and justify the use of the $E(^1L_a)$ abscissas of Figures 6 and 7.

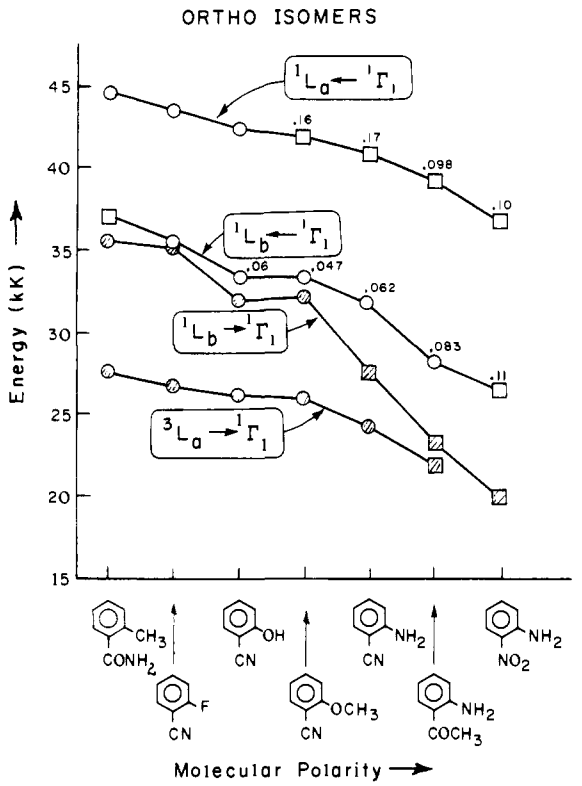

Figure 6. The absorption and emission data for ortho-disubstituted benzenes, arranged according to increasing molecular polarity as determined by decreasing $^1L_a \leftarrow {}^1\Gamma_1$ energy. The absorption data refer to nonpolar media (methylcyclohexane or 3-methylpentane) at room temperature; the emission data refer to glassy ethanol or EPA media at 77 K. The circles refer to band origins; the squares refer to band maxima. The superposed numbers are the oscillator strengths of the absorptive transitions. The data are taken from Table I of I.

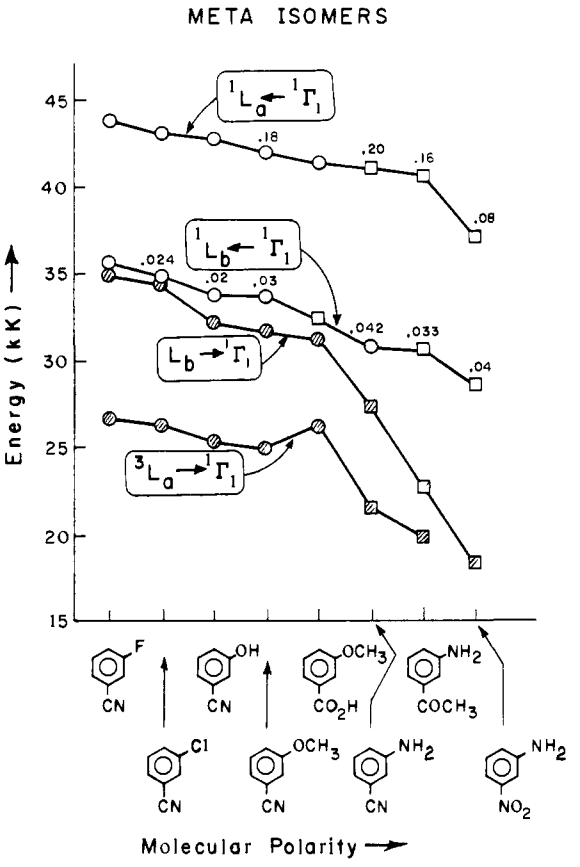

Figure 7. Absorption and emission data for meta-disubstituted benzenes, arranged according to increasing molecular polarity as determined by decreasing $^1L_a \leftarrow {}^1\Gamma_1$ energy. The absorption data refer to nonpolar media (methylcyclohexane or 3-methylpentane) at room temperature; the emission data refer to glassy ethanol or EPA media at 77 K. The circles refer to band origins; the squares refer to band maxima. The superposed numbers are the experimental oscillator strengths. The data are taken from Table I of I.

The trends evident in Figures 6 and 7 are essentially identical with those found in Figures 4 and 5. When Figures 1, 6, and 7 are analyzed in conjunction with Table II of I, we can draw certain generalizations about the absorption spectroscopic behavior. We label these generalizations A′, B′, C′, . . . , to distinguish them from the set A, B, C, . . . , deduced independently from the CNDO/s-CI results. We also imply a congruence of generalizations A and A′, B and B′, etc., in the sense that they signify the same physical result. The observed trends follow.

(1) A′ is congruent with A. The ^1L_b band of para always lies at higher energy than those of either ortho or meta. The opposite is true of the ^1L_a band. Both energy differences increase with both increasing D/A index and solvent polarity.

(2) B′ is congruent with B.

(3) For C′, the ^1L_a-^1L_b band gap remains relatively constant at 8000-1200 cm^{-1}. While somewhat erratic, the general tendency is one of slight increase with increasing D/A index. C′ is essentially identical with C.

(4) D′ is congruent with D.

(5) E′ is congruent with E. While it is rather difficult to make general statements about individual band intensities because of apparently erratic deviations, the following trends with increasing D/A index appear to obtain: $f(^1L_a)$ and $f(^1L_b)$ of both the orthos and metas decrease and increase, respectively, $f(^1L_a)$ of the paras increases, and $f(^1L_b)$ of the paras remains either constant or suffers a small increase.

(6) For F′, the vibronic structuredness of the spectra decreases with increasing D/A index and solvent polarity.

If Figures 2, 6, and 7 are analyzed in conjunction with Table III of I, we can draw certain generalizations about the emission spectroscopic behavior. These generalizations are labeled A″, B″, C″, . . . , to distinguish them from the sets of generalizations {A, B, C, . . .} and {A′, B′, C′, . . .} which were deduced independently. We also, by this labeling, imply a congruence, of a physical nature, of observations A, A′, and A″; B, B′, and B″; etc. The observed trends follow.

(1) A″ is congruent with A and A′.

(2) For B″, ^1L_a fluorescence is not observed, only ^1L_b fluorescence. Insofar as $E(^1L_b)$ is concerned, B″ is congruent with both B and B′.

(3) For C″, the luminescence spectra contain no information on the ^1L_a-^1L_b band gap, but the excitation spectra of either fluorescence or phosphorescence do. The excitation spectra confirm both C and C′, the band gap in most instances being ~10 000 cm^{-1}.

(4) D″ is congruent with D and D′. The use of excitation spectra is necessary to validation of this point.

(5) For E″, the only information on this point is contained in the intrinsic fluorescence lifetimes of Table II and these, unfortunately, do not permit any unambiguous statement.

(6) F″ is congruent with F′.

(7) For G″, the energy difference $E(^1L_b$, para) − $E(^1L_b$, ortho or meta) is positive and it increases with increasing polarity until $^1L_a/^1L_b$ crossover occurs in the para isomer. Thereafter, the fluorescence of the para derivative is of ^1L_a type and, with continuing increase of solute and solvent polarities, it may eventually achieve lesser energy than the ^1L_b fluorescence of either the ortho or meta isomer.

(8) For H″, the quantum yield ratio of phosphorescence to fluorescence, ϕ_p/ϕ_f, is largest in the para isomer. This characteristic is demonstrated in Table II. Fluorescence dominates

Table II. Luminescence Properties of a Representative Sample of D-Ph-A Molecules[a]

molecule	isomer	$\tau_f°$, 10^{-9} s	τ_p, s	ϕ_f	ϕ_p	ϕ_p/ϕ_f
fluorobenzonitrile	*o*	50	2.43	0.51	0.09	0.18
	m	46	2.60	0.54	0.08	0.15
	p	141	2.05	0.24	0.23	0.96
cyanoanisole	*o*	19	1.4	0.26	0.11	0.42
	m	23	1.8	0.21	0.09	0.45
	p		1.6	0.23	0.23	1.0
cyanoaniline	*o*	22	3.65	0.31	0.10	0.31
	m	15	2.65	0.87	0.05	0.05
	p	33	2.45	0.15	0.11	0.73
aminoacetophenone	*o*	20	0.06	0.58	0.08	0.14
	m	38	0.23	0.82	0.11	0.13
	p	480	0.72	0.11	0.14	1.3
nitroaniline	*o*			yes	~0	~0
	m			yes	~0	~0
	p		0.2-0.1[b]	~0	yes	~∞

[a] $\tau_f°$ denotes the intrinsic fluorescence lifetime; τ_p, the observed phosphorescence lifetime, in a glassy medium at 77 K; ϕ_f, the quantum yield of fluorescence; ϕ_p, that of phosphorescence. These data are taken from Lui and McGlynn [Y. H. Lui and S. P. McGlynn, *J. Lumin.*, **9**, 449 (1975); *J. Mol. Spectrosc.*, **55**, 163 (1975); *J. Lumin.*, **10**, 113 (1975); *Spectrosc. Lett.*, **11**, 47 (1978)]. [b] The value of τ_p is solvent dependent.

the emissivity of the ortho and meta isomers whereas, in the para isomer, the fluorescence and phosphorescence components prior to the $^1L_a/^1L_b$ crossover point are comparable. The major variations in ϕ_p/ϕ_f which occur in the para isomers in the crossover region are absent in the ortho and meta isomers, where there is no crossover.

(9) For I″, the T_1 state in all instances is the ^3L_a state.

(10) For J″, prior to the cross-over region of para, the solvent sensitivity of either ortho or meta fluorescence is greater than that of para. After the crossover region, the opposite is the case.

Discussion

The gamut of trends in the spectra of *o*- and *m*-D-Ph-A molecules as a function of D/A index, whether μ_0 or $E(^1L_a)$, have been elaborated both experimentally and computationally. The cohesion of the two data sets, computational and experimental, is remarkable. All that remains is to interrelate disparate trends so that the common factor influencing all of them becomes obvious.

The fluorescence of the ortho and meta isomers is always $^1L_b \rightarrow {}^1\Gamma_1$ and its cross section increases with decreasing $E(^1L_a)$. Consequently, in the absence of intervening $^{1,3}\Gamma_{n\pi^*}$ states, one expects that this cross-sectional increase will lead to a decrease of ϕ_p/ϕ_f, much as is observed. Similarly, since the cross section of $^1L_b \rightarrow {}^1\Gamma_1$ is always considerably higher in the ortho-meta pair than in the para isomer, one expects that ϕ_p/ϕ_f might be considerably larger in the para isomer, which, again, is the case experimentally.

The solvent sensitivities and vibronic-structural trends, noted above in several places, are mediated by solute-solvent interactions. In terms of the solvent shift data of Table III, we may conclude that the degree of CT in the various states is ^1L_a (para) > $^1L_{a,b}$ (ortho, meta) > ^1L_b (para) and that it increases in all states with increasing D/A index. (This conclusion is fully congruent with characteristic J″.) Hence, the solvent sensitivity will increase in the order ^1L_b (para) < $^1L_{a,b}$ (ortho, meta) < ^1L_a (para) and will be more extreme the more polar the solute. The lack of vibronic structure, then, is attributable to an ensemble of solute-solvent adducts of somewhat different geometries and degrees of coordination.

The existence of characteristic A′ is a consequence of the loss of the (possibly approximate) C_{2v} symmetry axis of the para isomer. This symmetry loss permits the input of strong $^1CT \leftarrow {}^1\Gamma_1$ dipole intensity and considerable CT character into both the $^1L_a \leftarrow {}^1\Gamma_1$ and $^1L_b \leftarrow {}^1\Gamma_1$ transitions of the ortho and meta isomers. In the para isomer, on the other hand, the input of both intensity and CT character is largely exclusive to the $^1L_a \leftarrow {}^1\Gamma_1$ transition. In other words, in the para isomer the allowed $^1CT/^1L_b$ mixing is restricted to higher energy CT states than those which mix with ^1L_a, and to CT states which have considerably smaller $^1CT \leftarrow {}^1\Gamma_1$ cross sections than those which mix with ^1L_a. Thus, the large intensity and energy dependence of the $^1L_a \leftarrow {}^1\Gamma_1$ transition of the para isomer on the D/A index is a result of the inability of the $^1L_b \leftarrow {}^1\Gamma_1$ transition of the para isomer to compete for low-energy, highly dipole-allowed CT character, an inability with which the $^1L_b \leftarrow {}^1\Gamma_1$ transition does not come encumbered in either the ortho or the meta isomers.

The phenomenological trends of Figure 2 are expected to hold as long as the configuration interactions of interest are principally confined to the three zero-order ^1L_a, ^1L_b, and ^1CT

Table III. Solvent Sensitivities of a Representative Sample of D-Ph-A Molecules

molecule	isomer	$-\Delta\bar{\nu}$, $\times 10^3$ cm^{-1} ($^1L_b \leftarrow {}^1\Gamma_1$)	$-\Delta\bar{\nu}$, $\times 10^3$ cm^{-1} ($^1L_a \leftarrow {}^1\Gamma_1$)
fluorobenzonitrile[a]	*o*	0.31	1.1
	m	0.38	1.1
	p	0.06	0.8
cyanoanisole[b]	*o*	0.34	
	m		1.46
	p	0.14	0.7
cyanoaniline[c]	*o*	1.1	0.9
	m	1.2	0.9
	p	<0.5	2.0
aminoacetophenone[c]	*o*	1.1	~1
	m	1.3	1.8
	p	<0.5	3.6
nitroaniline[c]	*o*	2.3	1.5
	m	3.7	2.7
	p		5.1

[a] $\Delta\bar{\nu}$ is defined as $\Delta\bar{\nu} \equiv E$(ethanol) − E(vapor) for the origin bands of the transition in question. [b] $\Delta\bar{\nu}$ is defined as $\Delta\bar{\nu} \equiv E$(ethanol) − E(methylcyclohexane) for the origin bands of the transition in question. [c] $\Delta\bar{\nu}$ is defined as $\Delta\bar{\nu} \equiv E$(ethanol) − E(3-methylpentane) for the band maxima of the transition in question. In the case of the para isomer, the $^1L_b \leftarrow {}^1\Gamma_1$ transition cannot be observed since it is occluded beneath the $^1L_a \leftarrow {}^1\Gamma_1$ absorption band. If the $^1L_b \leftarrow {}^1\Gamma_1$ transition had red shifted by 0.5×10^3 cm^{-1} or more in the ethanol solvent, it would have been observed. Hence, we can infer the maximum shift experienced in the para isomers of cyanoaniline and aminoacetophenone. In the case of *p*-nitroaniline, the $^1L_b \leftarrow {}^1A$ transition is not observable in either polar or nonpolar media.

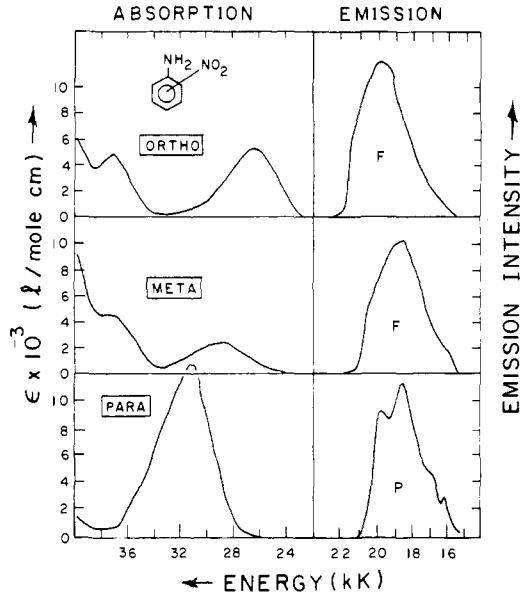

Figure 8. Absorption (left side, in methylcyclohexane solvent at 300 K) and emission (right side, in EPA glass at 77 K) spectra of the nitroanilines. The ortho/meta/para isomers are arranged in the order top/middle/bottom.

states. If, however, other additional zero-order $^1\Gamma_{\pi\pi^*}$ states are introduced in the appropriate energy regime so that further configuration mixing can ensue, major perturbations of the trends of Figure 2 can be expected. A case in point is provided by the nitroanilines of Figure 8. The D/A index of nitroanilines is such that it should fit on the extreme right of Figure 1 and, hence, the value of $\epsilon(^1L_a, \text{para})$ should be greater than 24 000 L/mol·cm. Its value, in fact, is only ϵ 13 000 L/mol·cm. This untoward decrease is connected with the introduction of locally excited (LE) states of the nitro group which are of an appropriate symmetry and energy to induce considerable ^{1}LE/^{1}CT/^1L_a mixing in the para isomer. The resultant diffusion of the large ^{1}CT $\leftarrow {}^1\Gamma_1$ intensity over a number of other transitions and the infusion of the small ^{1}LE $\leftarrow {}^1\Gamma_1$ intensity into the $^1L_a \leftarrow {}^1\Gamma_1$ transition is responsible for the observed decrease of $f(^1L_a, \text{para})$.

The absorptive properties of *p*-nitroaniline, as seen, provide a nice illustration of the effects of the introduction of a donor group which introduces ^{1}LE zero-order states of the appropriate energy and symmetry. However, once such a perturbation has been introduced, with further change of the conjugate group (as long as any such change does not itself introduce new zero-order states of the conjugate addendum which may also alter the existing CI situation) one expects the reoccurrence of the regular trend variation exhibited in Figure 1. An example is provided by the series D-Ph-NO_2. The phenomenological trends of Figure 2, so decisively disrupted by nitroaniline, are still fully present in the series D-Ph-NO_2. For example, the values of the extinction coefficient and the energy of the $^1L_a \leftarrow {}^1\Gamma_1$ transition of the para isomer in nonpolar media exhibit the regular variations shown in Table IV.

The introduction of low-energy $^1\Gamma_{n\pi^*}$ of LE type seems to have little effect on the absorption spectroscopic trends of Figure 1. Such states, for most common D and A groups, (1) are usually of very low intensity, (2) are strictly prohibited from CI mixing with (or, at least, confined to very weak CI mixing with) the zero-order ^1L_a, ^1L_b, and ^{1}CT set, and (3) usually lie at energies comparable to or higher than the ^1L_a, ^1L_b levels. As a result, the $^1\Gamma_{n\pi^*} \leftarrow {}^1\Gamma_1$ transition, when present, is usually occluded beneath the ^1L_a, $^1L_b \leftarrow {}^1\Gamma_1$ absorption bands and its presence is not detectable. This is certainly the case in the series

Table IV

D	ϵ, L/mol·cm	E, $\times 10^3$ cm^{-1}
CHO	1900	33.8
OH	9500	31.6
NH_2	13 000	26.8
$NHNH_2$	15 300	26.0
O^-	18 000	25.0

Table V

D	ϵ, L/mol·cm	E, $\times 10^3$ cm^{-1}
CN	1400	36.7
CH_3	1500	~36
OH	1600	~35
$N(CH_3)_2$	3300	31.4

D-Ph-NO_2 (see Figure 8 and the compilation of Table IV), the series D-Ph-$COCH_3$ (see Figure 1), and the series D-Ph-CHO (as witness the data compilation for the para isomers shown in Table V, in which no irregularities are evident).

The introduction of low-energy $^1\Gamma_{n\pi^*}$ states, however, does exert major influences on the luminescence characteristics. This topic was discussed in Appendix 1 of I, to which we refer the reader, and which we now elaborate in order to explain the luminescence oddities of Figure 8. The energies of the $S_1(\pi\pi^*)$ state in the nitroanilines are $E(S_1, \text{ortho}) \simeq E(S_1, \text{meta}) < E(S_1, \text{para})$; on the other hand, the energies of the $^{1,3}\Gamma_{n\pi^*}$ states of lowest energy are[10] $E(^{1,3}\Gamma_{n\pi^*}, \text{ortho}) \simeq E(^{1,3}\Gamma_{n\pi^*}, \text{meta}) > E(^{1,3}\Gamma_{n\pi^*}, \text{para})$. These two small differences, being additive in effect, provide the order $E(^3\Gamma_{n\pi^*}) < E(S_1)$ for the para isomer and $E(^3\Gamma_{n\pi^*}) > E(S_1)$ for the ortho and meta isomers. Thus, following the arguments of El-Sayed,[11] we can readily interpret the nonphosphorescence of the ortho and meta isomers and the nonfluorescence of the para isomers. Furthermore, we recognize that an increase of either the donor character of D in *p*-D-Ph-NO_2 above that of NH_2 or of solvent polarity should produce a decrease of $E(^1L_a, \text{para})$ and an increase of $f(^1L_a)$ so that one might pass from the situation $E(^3\Gamma_{n\pi^*}) < E(S_1)$ through $E(^3\Gamma_{n\pi^*}) \simeq E(S_1)$ to $E(^3\Gamma_{n\pi^*}) > E(S_1)$ and, hence, from a limiting situation of dominant phosphorescence to another of dominant fluorescence, the region between the limits being characterized by comparable fluorescence/phosphorescence intensities. Observations in accord with these predictions are available in the work of Khalil.[12] Concomitantly, a similar increase of either donor character for the ortho and meta isomers or of solvent polarity will not alter the existing situation $E(^3\Gamma_{n\pi^*}) > E(S_1)$ for the ortho and meta isomers and, hence, should not affect the luminescence properties of these isomers. Unfortunately, data for such systems are not available.

Acknowledgment. This work was supported by the U.S. Department of Energy—Physics and Technological Programs—Division of Biomedical and Environmental Research.

References and Notes

(1) The works of J. N. Murrell (Sheffield) and S. Nagakura (Tokyo) are synopsized in J. N. Murrell, "The Theory of the Electronic Spectra of Organic Molecules", Wiley, New York, 1963, and H. Suzuki, "Electronic Absorption Spectra and Geometry of Molecules", Academic Press, New York, 1967.
(2) The D/A index is a qualitative measure of the relative donor and acceptor strengths of the donor and acceptor substituents. It is explained in the previous paper (paper I), where means of quantifying it are also elaborated.
(3) I: T. P. Carsey, G. L. Findley, and S. P. McGlynn, *J. Am. Chem. Soc.*, preceding paper in this issue.
(4) See the procedure detailed in I.
(5) The off-axis component in *p*-cyanophenol is attributable to the nonsymmetric placement of the -O-H group (see Figure 1 of I).

(6) The molecular geometry was generated using standard bond-length and bond-angle values from J. A. Pople and D. L. Beveridge, "Approximate Molecular Orbital Theory", McGraw-Hill, New York, 1970, pp 111–112.
(7) A. C. Shapski and J. L. Stevenson, *J. Chem. Soc., Perkin Trans. 2*, 1197 (1973). Amino and phenyl hydrogen bond lengths and angles were taken from K. Trueblood, E. Goldish, and J. Donohue, *Acta Crystallogr.*, **14**, 1009 (1961).
(8) The oscillator strength of the transition $^1\Gamma_j \leftarrow {}^1\Gamma_1$ is referred to here and elsewhere as $f(^1\Gamma_j)$.
(9) T. P. Carsey, Ph.D. Dissertation, Louisiana State University, Baton Rouge, 1977.
(10) V. G. Plotnikov and V. M. Komarov, *Spectrosc. Lett.*, **9**, 265 (1976).
(11) M. F. A. El-Sayed, *J. Chem. Phys.*, **38**, 2834 (1963).
(12) O. S. Khalil and S. P. McGlynn, *J. Lumin.*, **11**, 185 (1975–1976).

Crystal and Molecular Structure of $[n\text{-}Bu_4N^+][S_3N_3^-]$ and the Vibrational Assignments and Electronic Structure of the Planar Six-Membered Ring of the Trisulfur Trinitride Anion

J. Bojes, T. Chivers,* W. G. Laidlaw, and M. Trsic

Contribution from the Department of Chemistry, University of Calgary, Calgary T2N 1N4, Alberta, Canada. *Received October 10, 1978*

Abstract: The crystal and molecular structure of $[n\text{-}Bu_4N^+][S_3N_3^-]$ has been determined by X-ray crystallography. The compound crystallizes in the space group $P2_1/n$, $a = 9.074$ (5) Å, $b = 15.901$ (12) Å, $c = 15.389$ (6) Å, $\beta = 98.98$ (4)°, $V = 2193$ Å^3, and $Z = 4$. The refined structure ($R = 0.097$) shows that the $S_3N_3^-$ ion is a six-membered, essentially planar ring with S–N distances in the range 1.580 (13) to 1.626 (12) Å. The bond angles within the ring at nitrogen are 122.6 (8)–124.2 (9)° and at sulfur they are 116.5–117.0 (7)°. The infrared and Raman spectra of alkali metal and tetraalkylammonium salts of $S_3N_3^-$ are discussed and assigned on the basis of D_{3h} symmetry for the anion. Ab initio Hartree–Fock–Slater SCF calculations have been carried out for $S_3N_3^-$ and show (a) that a planar configuration is of lower energy than other ring conformations and (b) that the ground-state electronic structure is a 10 π system with a net of one π bond distributed over the six S–N bonds of the ring. Assuming the corresponding cation, $S_3N_3^+$, to have a planar (D_{3h}) geometry, similar calculations predict this species to be a diradical. Calculations of the energy and oscillator strengths for the lowest allowed electronic transitions of $S_3N_3^-$ lead to the assignment of the 360-nm peak in the electronic spectrum to a $\pi^* \rightarrow \pi^*$ transition (calculated wavelength 399 nm).

Introduction

Recently the synthesis and characterization of cesium and tetraalkylammonium salts of the novel sulfur–nitrogen anion, $S_3N_3^-$, from the reaction of the appropriate azide with S_4N_4 in ethanol were reported.[1] The vibrational spectra of these salts suggested a six-membered ring structure for $S_3N_3^-$, in contrast to the five-membered ring structure established for the isoelectronic cation, $S_3N_2Cl^+$,[2] and also found in a number of S_3N_3 derivatives, e.g., $S_3N_3COCF_3$.[3] In the particular case of the cesium salt, we concluded from the vibrational spectra that the ring in $S_3N_3^-$ was puckered (C_{3v}).[1] Six years ago, in a discussion of his proposals for "electron-rich aromatic" S–N species, Banister wrote "it is not known whether an anionic charge (e.g. as in $S_3N_3^-$) has a serious destabilizing effect on sulphur d_π bonding, as no planar anions have been prepared."[4,5] Since a knowledge of the structure is an essential prerequisite to a discussion of the bonding in $S_3N_3^-$, an X-ray structural determination of $n\text{-}Bu_4N^+S_3N_3^-$ was undertaken and the details are reported here together with the vibrational assignments for the $S_3N_3^-$. In addition, we have carried out ab initio Hartree–Fock–Slater (HFS) SCF calculations of the ground-state electronic structure of $S_3N_3^-$ (and of the related cation $S_3N_3^+$) in order to (a) determine the relative energies of various ring geometries, (b) ascertain that the planar anion is a Hückel-type (10π) system, (c) assign the 360-nm band observed in the UV–visible spectrum of $S_3N_3^-$ to the appropriate electronic transition.

Experimental Section

Crystal Preparation. $[Bu_4N^+][S_3N_3^-]$ was prepared from tetra-*n*-butylammonium azide and S_4N_4 in ethanol, as previously described.[1b] Yellow prisms suitable for X-ray diffraction studies were obtained by the rapid evaporation (3–4 h) of a solution in absolute ethanol at 0 °C in a stream of nitrogen. The dimensions of the crystal used in this study were 0.3 × 0.3 × 0.35 mm. All manipulations were carried out under an atmosphere of dry nitrogen in view of the sensitivity of $S_3N_3^-$ salts to air oxidation, particularly in solution. In one attempted recrystallization of $[Me_4N^+][S_3N_3^-]$, during which an ethanol solution was allowed to stand for 24 h, white crystals of tetramethylammonium tetrathionate were obtained and identified by infrared bands at 1025 s, 620 s, 535 s, 525 s, 485 w, 460 w, and 370 w cm^{-1} and by elemental analysis. Anal. Calcd for $C_8H_{24}N_2S_4O_6$: C, 25.79; H, 6.51; N, 7.52; S, 34.42; O, 25.76. Found: C, 25.42; H, 6.71; N, 7.53; S, 34.41; O, 25.93 (by difference).

Crystal Data. $[Bu_4N^+][S_3N_3^-]$, mol wt 380.68, monoclinic. For calculation of cell constants, 25 reflections were computer centered and the setting angles were least-squares refined. The following systematic absences were observed: $h0l$, $h + l \neq 2n$; $0k0$, $k \neq 2n$. The cell constants are $a = 9.075$ (5) Å, $b = 15.901$ (12) Å, $c = 15.389$ (6) Å, $V = 2193$ Å^3, $Z = 4$, $d_c = 1.152$ g cm^{-3}, space group $P2_1/n$.

X-ray Measurements. Intensity data were collected at 23 ± 1 °C using graphite monochromated Mo Kα radiation ($\lambda = 0.710\,69$ Å) and a θ–2θ scan rate varying from 4 to 24°/min, depending on the intensity of the reflection. Stationary background counts with a time equal to half the scan time for each reflection were made at each end of the scan range. The scan range varied from −0.5° at low 2θ to +0.5° for the higher angle data. Of the 3951 reflections collected in the range $0° < 2\theta$ (Mo Kα) $< 50°$, 3374 unique reflections with $I > 3\sigma(I)$ were retained as observed and corrected for Lorentz and polarization effects. Three representative reflections were measured periodically to check crystal and electronic stability, but no significant change in intensity was observed. The linear absorption coefficient of this compound is 3.34 cm^{-1} for Mo Kα radiation and no absorption correction was necessary.

Solution and Refinement of the Structure. The structure was solved by direct methods. Using 312 reflections ($E_{min} = 1.40$) and 2000 phase relationships, a total of 16 phase sets were produced. An E map pre-

0002-7863/79/1501-4517$01.00/0